LBNL-51734

On Atmospheric Dispersion of CO_2 Seepage from Geologic Carbon Sequestration Sites

C.M. Oldenburg, A.J.A. Unger, and R.P. Hepple

November 2002

Earth Sciences Division
Ernest Orlando Lawrence Berkeley National Laboratory
Berkeley, CA 94720

BP–DOE CRADA
Health, Safety, and Environmental Risk Assessment for Leakage of CO_2 from Deep Geologic Storage Sites

Task 3. Report on atmospheric dispersion of CO_2 from leakage scenarios provided in Task 1.

This work was supported in part by a Cooperative Research and Development Agreement (CRADA) between BP Corporation North America, as part of the CO_2 Capture Project (CCP) of the Joint Industry Program (JIP), and the U.S. Department of Energy (DOE) through the National Energy Technologies Laboratory (NETL), and by the Ernest Orlando Lawrence Berkeley National Laboratory, managed for the U.S. Department of Energy under contract DE-AC03-76SF00098.

DISCLAIMER

TABLE OF CONTENTS

LIST OF TABLES

LIST OF FIGURES

EXECUTIVE SUMMARY

The transport of carbon dioxide (CO_2) by wind and density-driven flow above the ground surface delivers CO_2 to receptors such as plants, humans, and other animals. However, during this above-ground transport process, significant dispersion is likely thus diluting CO_2 concentrations to safe levels. While intuition suggests that mixing and dilution in the atmosphere will be fast processes, experience from natural CO_2 releases and industrial dense gas accidents demonstrates that dense gases resist mixing under certain circumstances. The purpose of this report is to summarize our work aimed at quantifying atmospheric dispersion of seeping CO_2 due to leakage from geologic carbon sequestration sites.

Carbon dioxide is a dense gas at ambient temperature and pressure relative to air (ρ_{CO2} = 1.8 kg m^{-3}, ρ_{air} = 1.2 kg m^{-3}). At ambient conditions, CO_2 is also 17% less viscous than air. The solubility of CO_2 in water is approximately 50 times larger than that of air, while molecular diffusivity of CO_2 in air is similar to that of other gases (~10^{-5} m^2 s^{-1}). These transport properties suggest that CO_2 can be very mobile as a dense gas flowing along the ground surface, and it will tend to dissolve in surface waters and rain, if present. Because potential CO_2 receptors such as plants, humans, and other animals live at or near the ground surface, our interest in atmospheric transport and dispersion is in the surface layer, the lowest part of which we refer to as the subaerial region, defined to be from the ground surface to an elevation of a few meters.

Numerous examples of natural hazardous releases of CO_2 gas have been documented. Natural emissions of CO_2 that have led to health risks have occurred from lakes in volcanic areas, low-energy fissure and flank volcanic eruptions, hydrothermal and cold springs, and vents in carbonate rocks and caves. While atmospheric dispersion likely dilutes natural emissions most of the time to nonhazardous levels, when factors such as topography and calm atmospheric conditions inhibit mixing, serious consequences including widespread death are known to occur.

Dense gases disperse differently from other gases in air due to the influence of the density contrast itself. In particular, a CO_2 cloud will tend to migrate downwards and thereby spread laterally on the ground. At moderate and low density contrasts, dense gases tend to resist mixing as density stratification inhibits turbulence. On the other hand, as spreading occurs driven by strong density contrasts, a dense gas cloud exposes more surface area to the ambient air across which mixing can occur.

Considerable research has been carried out on dense gas dispersion for health, safety, and environmental (HSE) risk assessment for industrial gases. Existing quantitative results of the behavior of dense gases upon release comes from field and laboratory experiments. Numerous useful empirical correlations have been developed that are applicable to CO_2 seepage. These correlations suggest that CO_2 will readily spread due to its high density. However, in the process of spreading in ambient winds, a CO_2 plume will mix and be diluted in a relatively short distance. Surprisingly, CO_2 plumes are predicted to be wider than they are long under conditions of light wind and strong source strength. Using these correlations and assuming an areal source with

length scale 180 m, we have come up with the following specific results for CO_2 seepage over flat land with sparse vegetation and no buildings:

- CO_2 seepage at rates on the order of 1 m^3 s^{-1} will tend to spread nearly 1 km under calm conditions in a one-hour period. If there are winds present, entrainment of ambient air will lead to extensive dispersion and dilution of the plume after a few hundred meters of travel downwind. The plume is predicted to be approximately as wide at the downwind end as it is long for winds of 1–5 m s^{-1} measured at an elevation of 10 m.
- CO_2 seepage at rates on the order of 0.1 m^3 s^{-1}, as investigated in Task 1 of this project, is expected to spread several hundreds meters in an hour under calm conditions. With winds of 1–5 m s^{-1} at 10 m elevation, CO_2 concentrations would be orders of magnitude smaller than initial concentrations approximately 100 m downwind, and the plume at this location would be twice as wide as it is long.
- At the smaller seepage rates (e.g., ~0.01 m^3 s^{-1}) investigated in Task 1 of this project, nearly complete dilution occurs after tens of meters of travel downwind, making HSE risks small to receptors present above ground.

Although the correlations are simple and derived from field and laboratory data, the conditions of the tests used in their derivation must be kept in mind when applying them more generally. In particular, topography and surface roughness may vary substantially from the ideal conditions relevant to the correlations. While the correlations suggest that mixing and dispersion will be effective in the surface layer, experience with natural CO_2 emission events suggests that careful consideration of local conditions is necessary.

Numerical simulation can be used to model more complex and site-specific features for CO_2 HSE risk assessment. Several different approaches of varying complexity are used to model atmospheric dispersion of dense gases as documented in the literature. Our review of the literature does not show any prior efforts to couple the subsurface and surface layer flow environments. In our approach, we model surface layer flow and dispersion with an advective-dispersive transport equation and a logarithmic velocity profile. Meanwhile, the subsurface flow and transport will be modeled using the standard multiphase version of Darcy's Law and advective-dispersive transport equation. Testing and development of this approach is ongoing. Preliminary results for a case of cold CO_2 seeping from the ground show that more testing and model development are needed.

1. INTRODUCTION

Of the many processes affecting carbon dioxide (CO_2) as it leaks from geologic carbon sequestration sites in the deep subsurface, migrates upwards through the saturated and unsaturated zones, and seeps out of the ground, transport and dispersion above the ground surface are perhaps the most important processes from the perspective of health, safety, and environmental (HSE) risks. Specifically, it is the transport of CO_2 above ground that will deliver CO_2, possibly in unhealthy concentrations, to receptors such as plants, humans, and other animals. However, during the process of this above-ground transport, significant dispersion is likely thus diluting CO_2 concentrations to safe levels. If atmospheric dispersion could always be counted on to disperse CO_2, HSE risk assessment could be focused solely on subsurface contamination, for example of ground water and the shallow subsurface root zone. However, experience with CO_2 emissions from volcanic and carbonate reservoir sources shows that lethal ground-hugging plumes of dense CO_2 gas have occurred regularly in the past. These natural occurrences of hazardous CO_2 emissions point to the need for careful consideration of above-ground transport and dispersion of CO_2 that may seep from man-made carbon sequestration reservoirs.

The purpose of this report is to summarize our work aimed at quantifying atmospheric dispersion of seeping CO_2 due to leakage from geologic carbon sequestration sites. The approach used parallels that of the Task 1 report (Oldenburg et al., 2002a) where we examined leakage and seepage. Namely we present first the relevant properties of CO_2, and then discuss the processes of atmospheric dispersion (Section 2). The discussion of properties and processes provides the background for understanding natural occurrences of CO_2 emissions that have led to severe consequences in the past (Section 3). Next we present empirical and scale analysis approaches, with application to the leakage scenarios we investigated in Task 1 (Section 4). We follow these results with a presentation of the state-of-the-art in atmospheric transport theory and modeling along with some preliminary test results from our own model (Section 5). We conclude with a summary (Section 6) of our findings related to the atmospheric dispersion of CO_2 relevant to potential seepage from geologic carbon sequestration sites.

2. PHYSICAL PROPERTIES AND PROCESSES

2.1 Density and Viscosity

In this section, we discuss the physical properties of carbon dioxide (CO_2) and the processes of dense gas dispersion. The emphasis is on the contrast in properties of CO_2 relative to air at ambient ground surface conditions. Carbon dioxide is a colorless and odorless gas with density approximately 1.9 kg m^{-3} at 1 bar, 10 ˚C. Shown in Figure 2.1 are the density and viscosity of CO_2-air mixtures as a function of composition at three different temperatures as calculated by the NIST14 database (NIST, 1992; Magee et al., 1994). As shown by the nearly linear mixing lines, the gases behave approximately ideally at atmospheric pressure. Note that the contrast in

density between CO_2 and humid air will be even larger because humid air is less dense than dry air due to the relatively smaller molecular weight of water (18.0 g mole^{-1}) relative to dry air (29.0 g mole^{-1}). In contrast to the density relative to air, CO_2 viscosity is lower than that of air as shown in Figure 2.1.

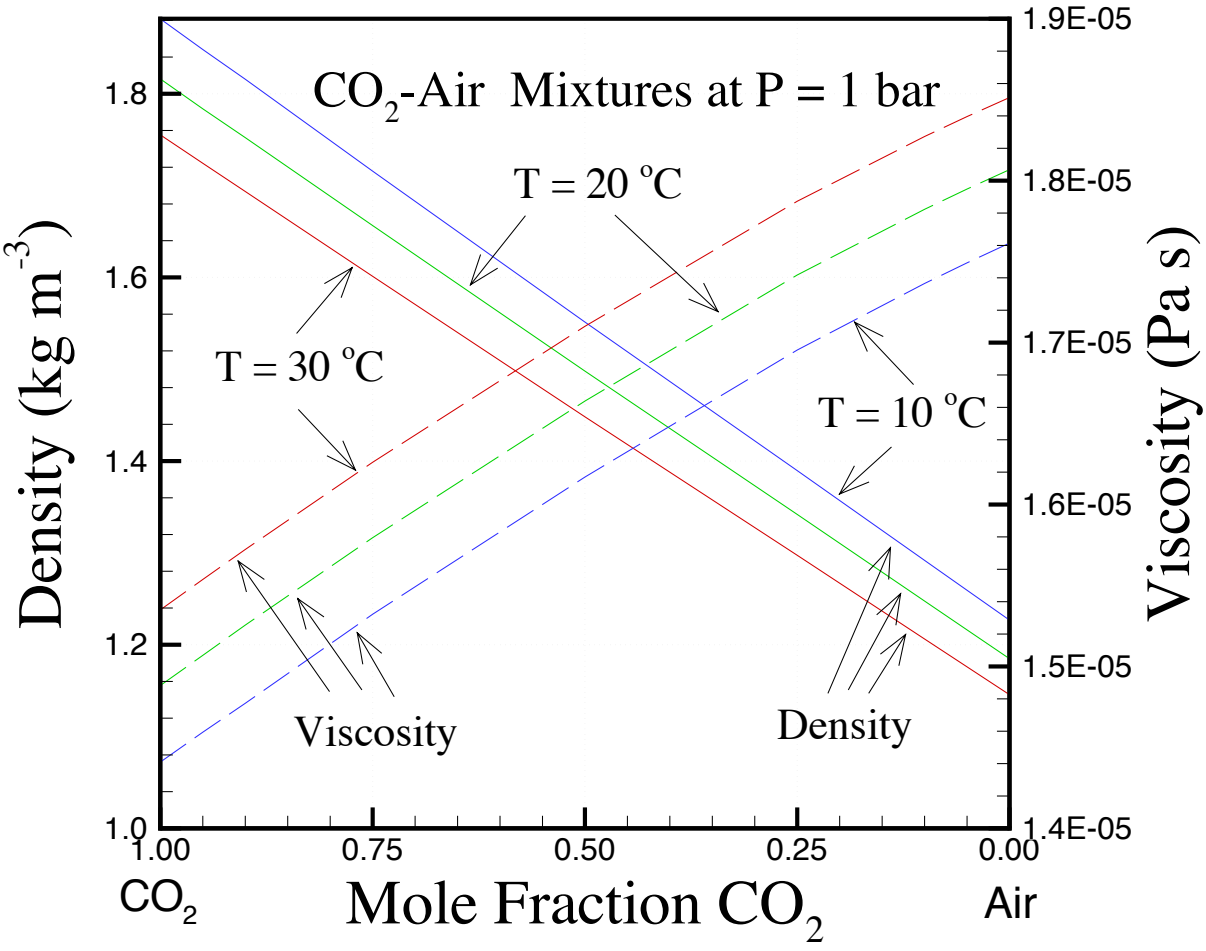

Figure 2.1. Density and viscosity of CO_2-air mixtures at 1 bar pressure and three different temperatures.

In addition to density and viscosity, the transport of CO_2 may also be influenced by molecular diffusivity in certain cases. The molecular diffusivity of CO_2 in air is comparable to other gases and is approximately 1.65 x 10^{-5} m^2 s^{-1} at 25 °C, 1 bar (Vargaftik et al., 1996). Carbon dioxide is relatively soluble in water, approximately 50 times more soluble than air (e.g., Cramer, 1982). Hence, surface waters and rainwater are capable of dissolving significant amounts of CO_2 when elevated concentrations are present.

2.2 Length Scales of Interest

Because HSE risks from seeping CO_2 will potentially occur to plants, humans and other animals at and near the ground surface, our focus is on CO_2 transport and dispersion in the region near the ground surface. This part of the atmosphere is formally referred to as the surface layer, defined as the lowest 10% of the atmospheric boundary layer that extends to an elevation of approximately 100 m (Stull, 1988). The stable boundary layer is in turn part of the planetary boundary layer which is on the order of 1 km thick. With the main HSE risks arising from exposure to high CO_2 concentrations near the ground surface, we refer to the shallowest part of the surface layer where the highest CO_2 concentrations are likely to be found as the subaerial environment. This terminology emphasizes that local topographic and surface roughness effects may allow dense gas with high CO_2 concentrations to resist atmospheric dispersion. As it is used here, the term subaerial environment denotes the region from the ground surface to an elevation of a few meters. It is not the intention of this study to consider mixing in the whole atmosphere or transport on length scales longer than approximately 1 km. The reason for our focus on the surface layer and relatively short lateral length scales is that this is where significant HSE risks due to high CO_2 concentrations are assumed to be encountered. Although we use the term atmospheric dispersion, we emphasize that our focus is on transport and dispersion in the surface layer and subaerial environment on much shorter length scales (e.g., site scale, $\sim 10^2$ m) than what the term often implies (e.g., continental scale, $\sim 10^6$ m).

2.3 Atmospheric Dispersion Processes

Atmospheric dispersion of gaseous components in ambient flows is generally very effective because the velocity field is spatially and temporally variable. Velocity variation gives rise to shear, entrainment, and turbulence, all of which act to decrease the length scale of gas clouds and correspondingly increase compositional gradients. With molecular diffusion of CO_2 and air at 1 bar and 20 ˚C on the order of 10^{-5} m^2 s^{-1}, once the length scale of a heterogeneity approaches a few millimeters in size, it can diffuse away on a 1 s time scale. Thus the processes of shear, entrainment, turbulence, and diffusion are fundamental to atmospheric dispersion.

One of the key aspects of atmospheric dispersion is whether or not the component being dispersed behaves actively or passively in the flow field. By active, we refer specifically in this report to the influence of CO_2 on the ambient flow field and mixing dynamics by virtue of the effect of CO_2 concentrations on gas density. Density differences between a dense gas and the ambient air affect dispersion and transport in at least four ways (Britter, 1989): (1) the velocity field produced by the horizontal density contrast is an additional driving force that must be considered along with the ambient flow; (2) the velocity gradient produced by these density-driven flows introduces shear that can lead to local turbulence and mixing between the two gases; (3) turbulence within the dense gas may be inhibited by density stratification; and (4) inertia arising from the release itself is dependent on the density contrast. The density contrast can also be such that the released gas is buoyant relative to air. For example, gases such as methane (CH_4) are lighter than air and will not lead to density stratification and the corresponding turbulence-

inhibiting effect. Thus light gases will mix readily as they rise in the atmosphere, perhaps explaining the difficulty in detecting seepage from leaking natural gas storage reservoirs (e.g., Allison, 2001).

For the case of passive gaseous components, the above effects are absent. For example, a low CO_2 flux corresponding to a night-time efflux of 10 μmole CO_2 m^{-2} s^{-1} (4.4 x 10^{-7} kg CO_2 m^{-2} s^{-1}) corresponding to a typical net ecosystem exchange (NEE) (Baldocchi and Wilson, 2001), typically does not increase CO_2 concentrations sufficiently to produce an active flow and will therefore mix passively even in gentle winds. In contrast, the release of CO_2 from a ruptured tank or pipeline can give rise to active flows as the concentrated and dense gas migrates along the ground surface driven by density effects and ambient winds. A volume of gas released in a short pulse from a tank is referred to as a cloud, whereas a continuously released volume of gas is referred to as a plume (Britter and McQuaid, 1988). Whether a given cloud or plume dispersal can be considered passive or active depends not only on the density contrast between the two gases, but also on the ambient wind velocity.

Note that many dense gases considered in the literature are actually lighter than air in terms of their molecular weight, but they are denser upon spilling because of their lower temperature. For example, liquefied natural gas (LNG) is liquid methane (CH_4), a lighter molecule than air (16.0 g $mole^{-1}$ vs. 28.96 g $mole^{-1}$), but it is transported and stored as a liquid at high pressure. Upon sudden release to ambient pressure, significant cooling associated with vaporization and expansion occurs and the gas cloud become denser than air by virtue of very low temperature. In contrast, CO_2 is heavier than air at ambient conditions (see Section 2.1). Similar expansion-related cooling processes to those of LNG will occur for supercritical or liquid CO_2 if it is released from tanks and pipelines into the ambient environment, but these releases are beyond the scope of the leakage- and seepage-related HSE risks being considered in this project.

3. EXAMPLES OF HAZARDOUS NATURAL CO_2 EMISSIONS

3.1 Introduction

Numerous examples of hazardous natural CO_2 emissions can be found in the literature, and far more undocumented examples are thought to exist. Significant overland transport occurs in many cases, and has caused widespread death in a number of dramatic events. In this section, we review some of the more well documented cases of CO_2 emission and overland transport relevant to the surface layer dispersion of CO_2.

3.2 Limnic Eruption of CO_2 from Lake Nyos, Cameroon

Lake Nyos, Cameroon, was the source of a large eruption of CO_2 that killed over 1700 people as gas flowed down narrow river valleys on the night of August 21, 1986 (Le Guern et al., 1992; Holloway, 2000). The reconstruction of events for Lake Nyos suggests that the degassing process lasted approximately four hours. A cloud of CO_2 believed to be in the range of 0.1–1.0 km^3 (1.9 x 10^8 kg to 1.9 x 10^9 kg) spilled out from the crater lake (Evans et al., 1994). For the

time period of four hours over which the emission occurred, the corresponding flow rate would have been 1.5–15 kg s^{-1} (0.8–8.0 m^3 s^{-1}). The gravity-driven mass quickly accelerated down the valleys comprising the drainage system of the lake. These long narrow valleys apparently prevented the cloud from dispersing. Within these valleys, people and animals were asphyxiated by the cloud over a distance of over 20 km from Lake Nyos. The minimal effects on vegetation and the absence of acid burns and severe eye irritation suggested the lack of any significant chemical components (e.g., H_2S) in the gas cloud aside from CO_2 and water. The cloud dispersed once it entered broader and more open valleys. The last people killed walked into low-lying or confined areas where CO_2 had collected and not yet dissipated (Baxter and Kapila, 1989; Barbieri et al., 1989; Faivre-Pierret et al., 1992).

3.3 Vents and Fissures, Dieng and Rabaul

Carbon dioxide releases from volcanic vents and fissures can be deadly. At the Dieng Volcanic Complex in Java, Indonesia, a series of earthquakes, eruptions, and lahars (debris flows) early in the morning of February 20, 1979, sent 142 inhabitants of Kaputjukan village fleeing toward the nearby town of Batur. They were later found sprawled out single file along a path where they had been overcome by volcanic gases released from fissures located 1 km upslope (Le Guern et al., 1982). As with other cases of rapid asphyxiation, there was no sign of any struggle or awareness of danger. The lack of any warning suggests that the gas was not visible and therefore composed mostly of CO_2. Later samples showed the gas to consist mostly of CO_2 with small amounts of H_2S. A few people apparently saw the others drop, went back to an elementary school in town for cover, and were overcome there. Later, several rescue workers were also killed by volcanic gas, bringing the final toll to 149 people. Many livestock and fish in local ponds were killed as well (Le Guern et al., 1982; Allard et al., 1989; Smithsonian Institute, 2001).

In another tragic event, six people were killed at Rabaul, Papua New Guinea, in the Tavurvur volcanic crater on June 24, 1990. The crater was a nesting ground for birds, and three people had entered the crater to collect eggs. The egg collectors were overcome by CO_2 that had built up inside the 25 m deep crater. Three more people died trying to rescue them. The CO_2 was passively emitted from a small vent in the wall of the crater. The height of the CO_2 pool ranged from 2 m to 5 m deep over the following few days. Observers noted that on windy days, the concentration of CO_2 in the crater was not lethal (Simkin and Siebert, 1994; Smithsonian Institute, 2001).

These two examples of vent and fissure emissions of CO_2 illustrate the hazard from low-energy eruptions. Specifically, CO_2 seepage that occurs without a large eruption of steam or volcanic ejecta has little energy available to cause advection, turbulence, and winds that can act to dissipate the cloud. The CO_2 in these cases never rises very high above the ground surface, and requires self-generated and ambient winds for its dissipation. Far more CO_2 is emitted in the short period of large volcanic eruptions, but along with the eruption comes eruptive energy that sends the cloud upwards and serves to dissipate hazardous gases.

3.4 Volcanic Degassing: Etna, Vulcano, and Mammoth Mountain

Mt. Etna in Italy accounts for a significant fraction of worldwide volcanic CO_2 emissions, and almost half is due to degassing along the flanks of the volcano (Allard, 1997; Gerlach, 1991). Vulcano Island, near Mt. Etna, is also known for significant gas emissions. Children and animals occasionally die near the volcano, probably from CO_2 asphyxiation (Baubron et al., 1990). These Italian volcanoes represent active volcanic systems that provide an opportunity to assess how people adapt to volcanic gas hazards and also to establish the relationship among release rates, surface topography, meteoric conditions, and hazard potential (Simkin and Siebert, 1994; Allard, 1997; D'Allessandro et al., 1997; Graziani et al., 1997).

The recent gas release at Mammoth Mountain in Long Valley caldera, California was associated with deep magmatic activity without concurrent surface volcanism. Not long after a swarm of earthquakes in 1989, large areas of dead trees were noticed, and a park ranger was overcome by CO_2 that had accumulated beneath snow. A series of investigations, primarily soil gas surveys, revealed that an enormous flux of CO_2 was passing up through the soil in the tree-kill areas and was well correlated with known fractures and faults (Farrar et al., 1995; Sorey et al., 1999; Rogie et al., 2001). Between 1990 and 1995, the total emission rate on the mountain was estimated to be greater than 1,200 tonnes CO_2 per day (14 kg s^{-1}). Soil gas concentrations at 10 cm depth in the tree-kill area were between 20 and 95% CO_2, versus less than 1% in soils outside of the high-flux zones. Since then, the average emission rate has diminished to several hundred tonnes per day or less in 1999 (Sorey et al., 1999; USGS, 1999). As much as 170 acres of forest have suffered tree-kill, and one skier apparently died from CO_2 asphyxiation in a snow well around a tree near Horseshoe Lake (Hill, 2000). This example demonstrates the potential for both human health and environmental impacts of high CO_2 concentrations in soil and snow.

3.5 Non-volcanic Emissions

Central Italy is well known for non-volcanic CO_2 emissions from vents and degassing from cold springs rich in CO_2 (e.g., Rogie et al., 2000). Of particular relevance to seepage from geologic carbon sequestration sites are the vents that emit CO_2 which then flows down topographic depressions effectively producing rivers of gas. These CO_2 flows kill small birds, rodents, and larger mammals who breathe the concentrated CO_2 gas in the stream. For example, at the Umbertide gas vent, the emission rate is approximately 0.1 m^3 s^{-1} (16 t day^{-1}), and dead animals are observed up to 50 m away in a topographic depression downstream from the vent (Rogie et al., 2000). The origin of the CO_2 is thought to be a combination of mantle degassing and decarbonation of limestone. Caves are another source of non-volcanic emissions, and some in Italy and Germany are called "dog's caves" because small animals are often killed in them by ground-hugging CO_2.

3.6 Hydrothermal Degassing

Geothermal and soda springs are concentrated in areas with active or quiescent volcanism and tectonic activity, but bicarbonate or CO_2-enriched springs occur in many groundwater systems. Aside from volcanic vents and fissures, geothermal and cold soda springs are the most common

manifestations of CO_2, and with rare exceptions, they pose little danger to humans or the environment (Brown, 1995; Barbier, 1997). Only when these springs seep into caves or near confined spaces do CO_2 levels build up to hazardous levels. Vegetation around soda springs shows no adverse effects, though some physiological adaptation to higher levels of CO_2 is likely (Stupfel and Le Guern, 1989; Reid et al., 1998; Pasquier-Cardin et al., 1999).

Travertine deposits are another common surface feature at high CO_2 discharge springs. High CO_2 groundwater in general and geothermal waters in particular dissolve carbonate and mobilize many cations in the subsurface and transport them to the surface (Duchi et al., 1987; Chafetz et al., 1991; Webster, 1995). When the high pCO_2 water reaches the atmosphere, CO_2 off-gases and disperses, then the resulting high pH carbonate-saturated fluid precipitates calcium carbonate (Pentecost, 1990, 1995; Chafetz et al., 1991). Travertine is a common consequence of CO_2 off-gassing, and it is associated with natural CO_2 accumulations that act as direct analogs for geologic containment (Ellis and Mahon, 1977; Allis et al., 2001).

3.7 Summary

Many examples of natural CO_2 emissions can be found on the continents. In many cases, emission rates are high and dispersion rates are low such that hazardous concentrations can arise leading to death of humans and other animals, as well as plants and trees. However, the vast majority of CO_2 emissions dissipate by mixing with ambient air and cause no significant local HSE risk. Having briefly discussed these natural analog cases of CO_2 seepage, we are now in a position to investigate the prediction of atmospheric dispersion relevant to CO_2 potentially seeping out of the ground from leaking geological carbon sequestration sites.

4. EMPIRICAL RESULTS FOR HEAVY GAS DISPERSION

4.1 Introduction

The widespread industrial use of gases and the occurrence of significant accidental releases have prompted extensive study of the transport and dispersion of dense gases. Excellent reviews of dense gas dispersion are provided in the review article of Britter (1989) and the monograph edited by Britter and Griffiths (1982). A recent special issue of *Atmospheric Environment* contains articles based on the Petroleum Environmental Research Forum (PERF) project on dense gas dispersion that was focused on model development using wind tunnel and field experimental results as constraints (Hanna and Steinberg, 2001). Most of the work on dense gas dispersion has relied on experimental results and correlations because simulating atmospheric flows is very difficult, and even when simulations can be carried out, validation of the models is difficult.

The main motivation for prior research on dense gas dispersion was HSE risk assessment of spills of dense industrial gases such as liquefied propane gas (LPG) (e.g., Britter, 1989). These studies have consisted of carefully monitored and controlled full-scale releases and bench-scale laboratory experiments, followed by dimensional and scale anaysis of the results to produce general correlations. The workbook of Britter and McQuaid (1988) provides a comprehensive

set of correlations and results applicable to dense gas dispersion. Although the correlations must be used with caution, they are thought to be good to approximately a factor of two (Britter and McQuaid, 1988). In some cases, the gases of interest are lighter than air by molecular weight (e.g., liquefied natural gas), but they are transported and stored at very high pressures to maintain liquid properties. Upon rupture of a tank or pipe containing such a liquid or supercritical gas, the decompression causes rapid cooling that results in a cold, dense gas phase relative to ambient air.

The motivation for the current work in this project is HSE risk assessment of CO_2 seeping out of the ground due to unexpected leakage from geologic carbon sequestration sites. As such, the complex heat transfer effects associated with liquid and supercritical gases flashing to vapor are not relevant to CO_2 seepage, as these decompression processes will have occurred at depth during migration upward to the ground surface. Because CO_2 can seep out of the ground at highly variable rates and under variable conditions, transport of CO_2 in the surface layer can occur either as a dense gas at high concentrations near the source or as a passive gas at low concentrations, e.g. farther downwind from the source. In both cases, the CO_2 is transported by advection and dispersion and may be influenced by wind blowing over the ground surface.

4.2 Criteria for Transport as an Active Gas

Based on the studies of Britter and McQuaid (1988), the following criterion for active versus passive behavior of gas mixing has been developed. For the case of a continuous source, the gas flow is passive if

$$\frac{\left(\frac{g'_0 q_0}{D}\right)^{1/3}}{U_{ref}} \leq 0.15 \qquad (4.1)$$

where q_0 is the volumetric flow rate ($m^3\ s^{-1}$), D is the source dimension (m), and U_{ref} is the ambient reference velocity ($m\ s^{-1}$) at height of 10 m averaged over 10 minutes, and g'_0 is the reduced gravity term, defined as

$$g'_0 = g\left[\frac{(\rho_0 - \rho_a)}{\rho_a}\right] \qquad (4.2).$$

In Eq. 4.2, g is the acceleration of gravity ($m\ s^{-2}$), ρ_0 is the density ($kg\ m^{-3}$) of the pure dense gas (e.g., CO_2), and ρ_a is the density of the ambient air ($kg\ m^{-3}$). Equation 4.1 can be modified by multiplying top and bottom by ρ/D^2 to express the criterion in terms of mass flux, where we assume the source area is of order D^2. By this assumption, the criterion becomes

$$q_{mf} \leq \frac{\left(0.15\, U_{ref}\right)^3 \rho_0}{D\, g\left(\frac{\rho_0 - \rho_a}{\rho_a}\right)} \tag{4.3}$$

We have plotted this function in Figure 4.1 assuming D = 100 m, ρ_0 = 1.9 kg m^{-3}, ρ_a = 1.2 kg m^{-3}. As shown in 4.1, the ambient reference velocity strongly controls whether the flow is passive or active. For example, from 1 m s^{-1} to 4 m s^{-1}, the flux will have to increase by a factor of 100 for the flow to remain active. For fluxes of the order of the Net Ecosystem Exchange (NEE) of 10 μmole CO_2 m^{-2} s^{-1} corresponding to 4.4 x 10^{-7} kg CO_2 m^{-2} s^{-1} (Baldocchi and Wilson, 2001), the transport will be passive for all but the smallest ambient velocities. In summary, CO_2 gas dispersion will be active for large fluxes and anytime the wind is light, as at night or in low-lying and protected areas.

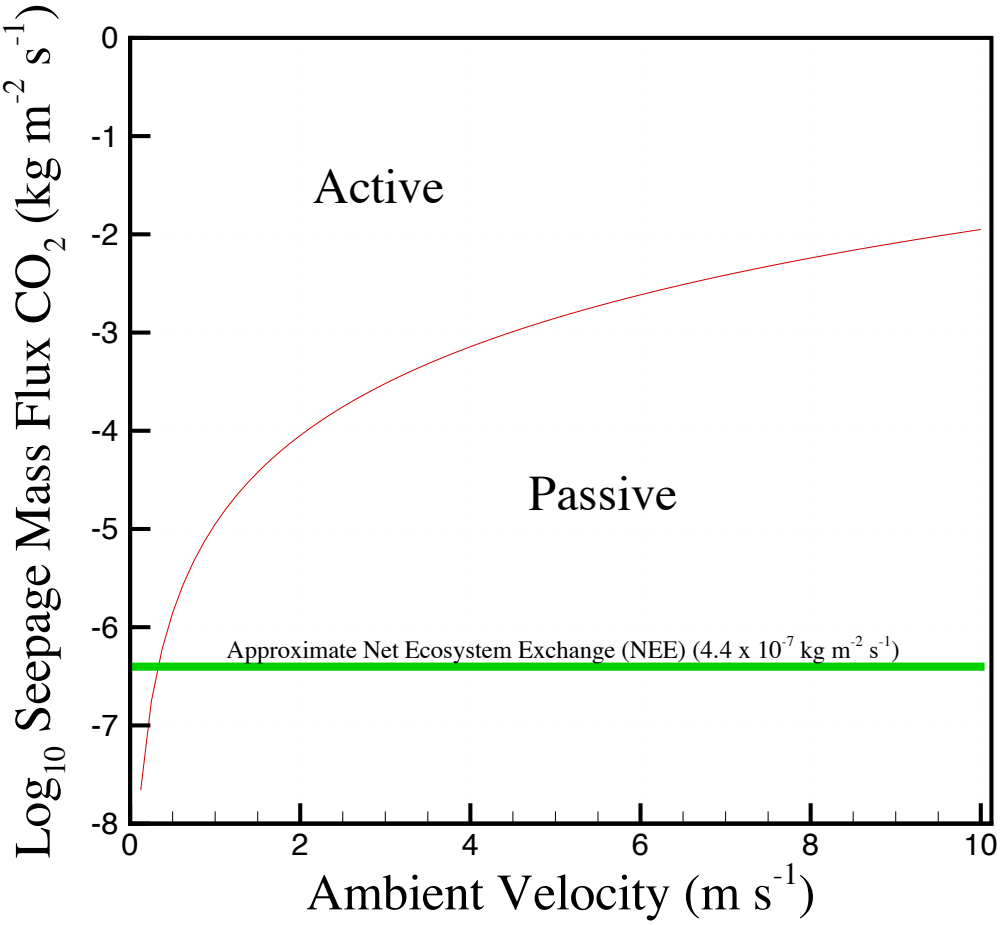

Figure 4.1. Criterion for active (density-dependent) flow as a function of seepage mass flux and ambient wind velocity.

4.3 Empirical Results of Plume Growth and Dispersion

In this section, we apply the correlations presented in Britter (1989) and Britter and McQuaid (1988) to cases of the dispersion of CO_2 plumes. In addition to the assessment of passive vs. active flow behavior described in Section 4.2, Britter and McQuaid (1988) provide additional correlations that are useful in predicting the flow and dispersion of CO_2 seeping from the ground surface. In particular, Britter (1989) presented a correlation for the radial spreading of a dense gas in the case of perfectly calm conditions and flat topography. This correlation is given as

$$r \approx \left(g'_0 q_0\right)^{1/4} t^{3/4} \qquad (4.4),$$

where r is the plume radius in meters, g'_0 and q_0 are defined in Section 4.2, and t is given in seconds. Another useful correlation relates the dispersion length, that is the distance at which the leading edge of the plume at a distance x_n from the source has a given concentration relative to the concentration at the source (Britter and McQuaid, 1988). The correlation is given in Eq. 4.5, where the function F is derived from data from actual field-scale releases of dense gas and is plotted in Figure 8 of Britter and McQuaid (1988):

$$\frac{x_n}{\left(q_0 / U_{ref}\right)^{1/2}} = \mathrm{F}\left(\left(\frac{g'_0{}^2 q_0}{U_{ref}{}^5}\right)^{1/5}\right) \qquad (4.5).$$

A simplified conceptual model is sketched in Figure 4.2 to clarify the various terms in Eq. 4.5. As shown, the plume is caused by a contiuous source (q_0), with advection caused by density effects and the ambient reference wind velocity of 2 m s^{-1} and reaches a dilution distance, x_n. As discussed in Britter and McQuaid (1988), the function F takes into account the decreased mixing that occurs due to density stratification when density contrasts are small to moderate, as well as the increased mixing that occurs when density contrasts are so large that significant density-driven flow leads to increased shear, turbulent eddies, and large increases in surface area as the dense plume spreads laterally. Note that viscosity, diffusivity, surface roughness, atmospheric stability, and source dimension are all absent from Eq. 4.5. Britter and McQuaid (1988) found that these factors are relatively unimportant in controlling dense gas dispersion.

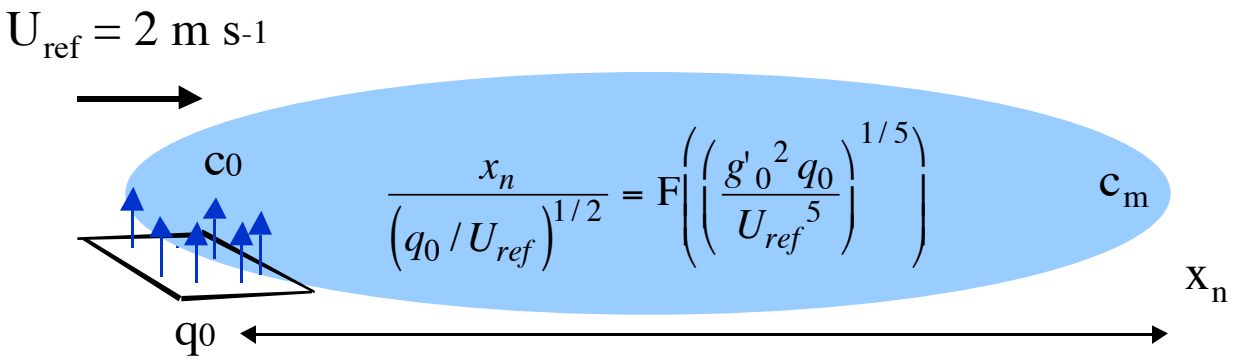

Figure 4.2. Conceptual sketch of plume with continuous source q_0 and downstream concentration c_m shown with the Britter and McQuaid (1988) dilution-distance correlation.

Britter and McQuaid (1988) offer additional correlations for plume extent. With reference to Figure 4.3, correlations are presented for the upstream migration (L_u), the lateral extent (width) at the source (L_{H0}), and the lateral extent (width) at any distance downstream (L_H) in terms of the source length scale (D), distance downstream (x), source flow rate (q_0), reduced gravity (g_0'), and buoyancy ratio of the plume (l_b) as follows:

$$L_u = \frac{D}{2} + 2\,l_b \qquad (4.6).$$

$$L_{H0} = D + 8\,l_b \qquad (4.7)$$

$$L_H = L_{H0} + 2.5\,l_b{}^{1/3} x^{2/3} \qquad (4.8)$$

$$l_b = \frac{q_0 g_0{}'}{U_{ref}{}^3} \qquad (4.9).$$

As shown in Eq. 4.6 and in Figure 4.3, the plume is expected to migrate upstream as well as spread laterally. Again we emphasize that these correlations are derived from experiments conducted under idealized conditions and do not consider special circumstances such as topography. Nevertheless, the correlations provide a general estimate of what can be expected in terms of plume spreading and dilution.

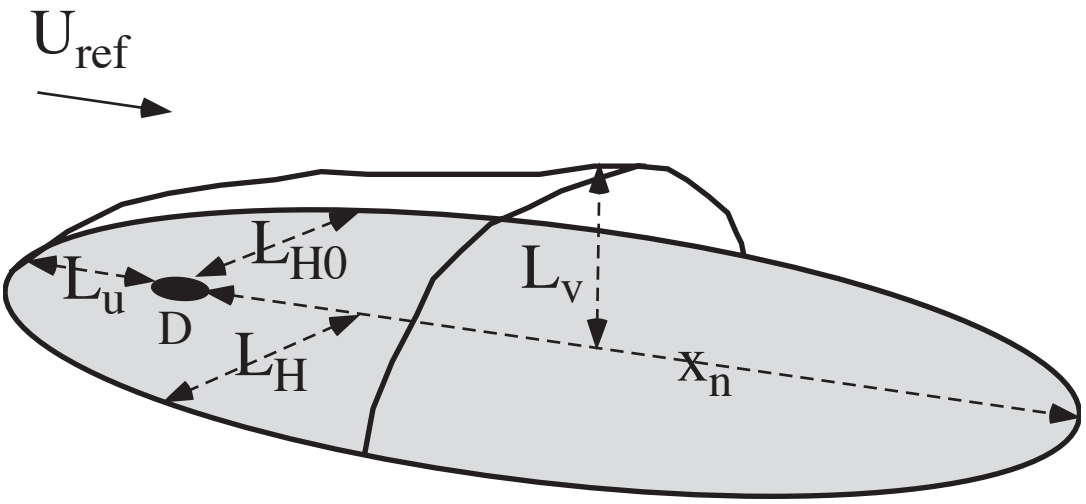

Figure 4.3. Three-dimensional sketch of plume conceptual model showing source length scale (D) and width (L_H), height (L_v), and length to an arbitrary concentration (x_n).

4.4 Application of Dense Gas Dispersion Correlations

In Task 1 of this project, we simulated the upward flow of leaking CO_2 in a model unsaturated zone. The leakage rates we used were plausible for slow leakage from deep carbon sequestration sites. In this section, we use the correlations of Britter (1989) and Britter and McQuaid (1988) to evaluate various aspects of the plume geometry for flow and dispersion of CO_2 seeping out from the ground.

Results are shown in Tables 4.1 and 4.2 for the correlations in Eqs. 4.1, 4.4, 4.5, 4.6, 4.7, and 4.8 for various CO_2 seepage rates, times, and wind velocities. It is important at this point to distinguish carefully between seepage and leakage. Leakage is migration away from the carbon sequestration target formation, while seepage is migration across the ground surface into the surface layer. Leakage was specified in the Task 1 report (Oldenburg et al., 2002a) in terms of the mass percentage of CO_2 that migrated away per year from a 4 x 10^9 kg carbon sequestration site. In our Task 1 work, the seepage rate was approximately equal to the leakage rate for the highest leakage used (0.1%/year), whereas for the lowest rate (0.001%/year) the seepage was approximately 20% of the leakage. This reduction in seepage as percentage of leakage is due to the attenuation occurring in the unsaturated zone, for example by spreading in the unsaturated zone and by rainfall infiltration dissolving excess CO_2 and carrying it downward to the water table. To examine a wide range of seepage scenarios including cases of high seepage rates or cases where barometric pumping enhances seepage (e.g., Rogie et al., 2001), we consider here a wide range of seepage rates from 10%/year down to 0.01%/year of the generic 4 x 10^9 kg carbon sequestration site. We chose the concentration ratio c/c_0 equal to 0.002, where c is concentration and c_0 is the initial concentration, as the ratio at which the plume has effectively dispersed to define the dilution distance.

The radial spreading results shown Table 4.1 show that spreading due to density contrast is a fast process. For example, a seepage flow rate of 0.67 m^3 s^{-1} will produce a 650 m radius plume in one hour, and a 7 km plume in one day according to the correlation of Eq. 4.4. This correlation assumes flat topography and smooth surface, and clearly must be used with caution for actual CO_2 plumes that occur over rough ground surfaces and are affected by ambient winds. In particular, many other processes are likely to affect the plume over these length scales, and the assumption of calm conditions inhibits significant dispersion. In short, we conclude from this correlation simply that density-driven gas flow is fast, and we can expect the tendency for CO_2 plumes to spread due solely to the CO_2-air density contrast even under calm conditions. This conclusion is consistent with intuition and experience as CO_2 and air are relatively inviscid, yet the density contrasts driving such flows are strong.

The third column in Table 4.2 shows that all of the flows are active insofar as density-dependence is concerned, except for the lowest seepage rates. At average ambient reference velocity greater than 10 m s^{-1} at an elevation of 10 m, many of these flows would become passive. The upwind plume extent shown in column four of Table 4.2 shows that upwind migration is a significant effect at high flow rates and low ambient velocities. Note that in Eqs. 4.6–4.8, we have assumed a source length scale of 177 m, which is an equivalent square dimension of a 100 m-radius circle such as we used for the source region of the simulations in Task 1 (Oldenburg et al., 2002a). The repeating upwind migration values of 89 meters in Table 4.2 indicate simply that the buoyancy is too small to contribute to upwind migration and the upwind distance is simply one half of the source length scale. Dilution distances in Table 4.2 show that wind speed controls atmospheric dispersion of dense CO_2 plumes. At low wind speeds, plumes can migrate a significant distance before dispersing, depending on the strength of the source flow rate. When the flow rate is small, the dilution is very fast since there is very little CO_2 available to affect gas density. At the high flow rates, the mixing lengths are significantly longer (e.g., 830 m, for 1 m s^{-1} wind). The width at the source shown in column 5 of Table 4.2 shows the tendency for dense gases to migrate laterally due to density effects. At high wind speeds or when the flow rate is low, the width reduces to the source width (177 m). The width of the plume at the dilution distance is shown in column 6. Again, we note the large lateral migration that is observed to occur for dense gases. For example, for the highest flow rate case with 1 m s^{-1} reference velocity, the lateral spreading is 50% larger than the dilution distance. When the reference velocity is increased to 10 m s^{-1}, the lateral spreading is 60% of the dilution distance. This tendency for the plume to migrate due solely to density gradients was already shown in Table 4.1, and this effect extends to lateral migration during downwind transport. When the widths show repeating values of 180 m in Table 4.2, it simply shows that there is no spreading beyond the extent of the source region with length scale 177 m.

It is interesting to note that the radial spreading and dilution distance correlations of Britter and McQuaid (1988) discussed here are given in terms of flow rate (units of m^3 s^{-1}) instead of mass flux (units of kg m^{-2} s^{-1}). The reason for this is that Britter and McQuaid (1988) found that the plume dispersion is a much stronger function of flow and dispersion processes than of the source geometry and size. To make usable correlations, Britter and McQuaid (1988) endeavored to minimize the number of variables in the correlations, hence the neglect of dependence on source

geometry in the correlation. This assumption is important to keep in mind when using the correlations in Table 4.1 and 4.2. Specifically, the very small dilution distances for the low seepage rates are probably not applicable since the source area for seepage is likely going to be larger than this distance, unless the seepage is occurring through a borehole, fault, or isolated preferential flow path of limited spatial area. We also note that all of the Task 1 simulation results were carried out in a radial geometry, whereas the dilution distance correlation requires a two- or three-dimensional Cartesian space to accommodate the unidirectional reference velocity.

Although the correlations of Britter and McQuaid (1988) are approximate, their application to the seepage rates of Task 1 (Oldenburg et al., 2002a) as shown in Tables 4.1 and 4.2 appear plausible. Together, the correlations imply that density-driven flow can be very fast, but that the plume does not migrate very far before significant dilution occurs. This suggests that atmospheric dispersion of CO_2 seeping from the ground is relatively effective at diluting CO_2 concentrations. However, the correlations assume that the ground is relatively flat and does not consider the effects of valleys and ridges. As is clear from Section 3, there are many examples of natural CO_2 plumes that do not disperse while traveling significant distances. Applying the dilution distance correlation to the Lake Nyos event asuming a flow rate of 4 m^3 s^{-1} (see Section 3) shows that the dilution length should be on the order of 1 km, yet the plume traveled over 20 km. Clearly there are other factors, for example topography and calm conditions, that can strongly inhibit the atmospheric dispersion of CO_2. These additional factors suggest that modeling approaches that go beyond simple empirical methods or one-dimensional parameterized equations are needed to assess in a defensible way the HSE risks of CO_2 seepage at any particular site.

Table 4.1. Radial spreading as calculated from Eq. 4.4.

CO_2 Seepage Rate	Radial Spreading (no wind)	
	time	radius [m]
10% / year or 6.7 m^3/s	100 sec	78
	1 hr	1100
	1 day	12000
1% / year or 0.67 m^3/s	100 sec	44
	1 hr	650
	1 day	7000
0.1% / year or 0.067 m^3/s	100 sec	25
	1 hr	360
	1 day	4000
0.01% / year or 0.0067 m^3/s	100 sec	14
	1 hr	200
	1 day	2200

Table 4.2. Plume characteristics as estimated from correlations.

CO_2 Seepage Rate	Correlation Results					
	Wind Velocity [m s^{-1}]	Active (A) vs. Passive (P)	Upwind Extent [m]	Dilution Distance x_n $c/c_0 = 0.002$ [m]	Width at Source Position [m]	Width at Dilution Distance x_n [m]
10% / year or 6.7 m^3/s	1	A	165	830	480	1200
	2	A	98	800	210	580
	5	A	89	640	180	300
	10	A	89	370	180	220
1% / year or 0.67 m^3/s	1	A	96	330	210	390
	2	A	90	300	180	270
	5	A	89	180	180	200
	10	A	89	110	180	190
0.1% / year or 0.067 m^3/s	1	A	89	124	180	220
	2	A	89	97	180	200
	5	A	89	47	180	180
	10	A	89	33	180	180
0.01%/year or 0.0067 m^3/s	1	A	89	44	180	190
	2	A	89	28	180	180
	5	P	89	14	180	180
	10	P	89	10	180	180

5. MODELING CO_2 TRANSPORT AND DISPERSION

5.1 Introduction

This section describes the state of the art in atmospheric dispersion modeling and presents initial results of our modeling studies. The purpose of this section is to present the current practice as the motivation for the approach that we are taking to model CO_2 flow and dispersion in a coupled subsurface-surface layer system. In this coupled approach, CO_2 will be able to seep out of and back into the ground surface. Some of the material below was already presented in the Task 2 report (Oldenburg et al., 2002b) in nearly the same form, but we have included it here again with updates to make the discussion complete.

5.2 Transport of Dilute CO_2 as a Passive Gas

Transport of CO_2 as a passive gas implies that it advects and disperses in the atmosphere without influencing the flow field (see Section 4). In order for this assumption to hold, CO_2 must be at sufficiently low concentrations that it does not affect the density of the ambient atmosphere. Under this assumption, we discuss below the underpinnings of the use of an ambient wind profile as well as advection and dispersion in the lower layers of the atmosphere as developed in the atmospheric transport literature (Slade, 1968; Arya, 1999; Pasquill, 1974).

The ambient time-averaged wind profile has been shown theoretically to follow a logarithmic profile. An excellent review of the assumptions and calculations involved in the logarithmic profile, as well as experimentally derived parameters obtained from calibration to field data is provided in Slade (1968). The logarithmic wind profile is given as:

$$u(z) = \frac{u_*}{k*} \ln\left(\frac{z}{z_0}\right) \tag{5.1}$$

where $u(z)$ is the ambient wind velocity as a function of elevation, u_* is the friction velocity, $k*$ is a regression parameter governing the wind profile near the earth's surface for various surface types, z is the elevation, and z_0 is a regression parameter representing the elevation at which $k*$ is measured.

Transport of CO_2 as a passive gas in the ambient atmosphere follows the linear advection-dispersion equation. A general background including all assumptions in the formulation of this equation can be found in Slade (1968) and Arya (1999). In general, this process can be simplified to the following partial differential equation for the three-dimensional (x, y, z) transport of a component (such as CO_2) at concentration c:

$$\frac{\partial c}{\partial t} + u_x \frac{\partial c}{\partial x} + u_y \frac{\partial c}{\partial y} + u_z \frac{\partial c}{\partial z} - D_{xx} \frac{\partial^2 c}{\partial x^2} - D_{yy} \frac{\partial^2 c}{\partial y^2} - D_{zz} \frac{\partial^2 c}{\partial z^2} = 0 \qquad (5.2)$$

In terms of atmospheric transport modeling, the coordinate system is arranged so that x is aligned in the downwind direction. Advection is generated by the velocity terms so that with the coordinate system transformation, $u_y = u_z = 0$, and u_x is the ambient wind profile. Dispersion is governed by D_{xx}, D_{yy} and D_{zz} which are the diagonal elements of a dispersion tensor and are related to the standard deviation in the concentration distribution by

$$\begin{aligned} \sigma_x^2 &= 2D_{xx}t \\ \sigma_y^2 &= 2D_{yy}t \\ \sigma_z^2 &= 2D_{zz}t \end{aligned} \qquad (5.3)$$

where t is time. The empirically derived Pasquill-Gifford (P-G) dispersion curves provide a commonly accepted and practical means of determining atmospheric dispersion, and are discussed in detail in Slade (1968) and Arya (1999). Essentially, large-scale eddies in the convective motion of the lower atmospheric layers are assumed to result in dispersion of passive constituents within these layers which can mathematically be represented as a Fickian diffusion process. Alternative empirical dispersion approaches which also rely on a Fickian diffusion representation of large-scale eddies in the lower atmosphere include the Brookhaven National Laboratory (BNL) Scheme as well as the Tennessee Valley Authority (TVA) Scheme (see Slade, 1968; Arya, 1999). The P-G scheme was developed from experiments conducted over a wide variety of terrain (e.g., project Prairie Grass and British diffusion experiments (Pasquill, 1961; Gifford, 1961)) and atmospheric conditions (ranging from extremely unstable, to neutral, to moderately stable) and therefore has received more attention than the BNL and TVA schemes which were developed under more limited conditions for site specific issues. The P-G curves provide a value of σ_y and σ_z as a function of downwind distance under a specific atmospheric condition, with σ_x set equal to zero.

The empirically derived P-G dispersion scheme is based on large-scale experiments and is valid for large-scale eddies in the lower atmospheric layers evolving at distances ranging from 100 m to 10,000 m downwind from the source. In the context of CO_2 transport, the source zone typically represents a surface seep and HSE risk issues resulting from the transport of CO_2 from this source zone need to be resolved at downwind distances up to 100 m from the source. At this scale, small-scale eddies in the convective motion of the near surface atmospheric layers are assumed to result in dispersion of passive constituents within these layers. These eddies are assumed to arise from the shear stress resulting from the viscosity of the air in contact with the ground surface. Note that this identical mechanism is responsible for the logarithmic wind profile discussed earlier, in which wind velocities approach zero at the ground surface. The Smagorinski

Model is the simplest and most widely used small-scale eddy dispersion model and is described in detail by Arya (1999). In general, the Smagorinski model provides a methodology to evaluate a dispersion tensor for use in the conservation of momentum equation when using the Navier-Stokes equations with a generalized anelastic approximation to model the flow of the atmosphere at the ground surface. Essentially, the dispersion of momentum is assumed to be proportional to the vertical and horizontal gradient in air velocity. Scalars such as a passive tracer or heat (energy) are assumed to undergo Fickian diffusion where the dispersion tensor is identical to that used in the momentum equation but multiplied by a constant ranging from 2.0 to 3.0.

In summary, the most commonly accepted and practical means of modeling large-scale atmospheric transport of CO_2 as a passive gas involves solving the 3-D advection dispersion equation for various source conditions of CO_2, $c(x, y, z, t = 0)$, with advection obtained from the logarithmic wind profile and dispersion obtained using the P-G dispersion curves. Within the immediate vicinity of the source zone, the same approach can be used with the dispersion coefficient estimated by the Smagorinski Model. Because Fickian diffusion is a linear flux operator in the context of the advection-dispersion equation, both the P-G and Smagorinski models can be used simultaneously with the largest dispersion term dominating dispersive transport.

5.3 Transport of Concentrated CO_2 as a Dense Gas

Advection of a dense gas plume is controlled by both the momentum imparted by the release rate as well as buoyancy forces due to the higher density of the gas relative to the ambient atmosphere. This density-driven flow produces a plume or cloud with, generally, an increased horizontal, and reduced vertical, extent when compared with a similar release having no density difference. The variation of density in the vertical direction will be stably stratified and turbulence and turbulent mixing can be significantly reduced or entirely inhibited. The velocity shear introduced by the density-driven flow may lead to intermingling of the dense gas plume with the ambient atmosphere and eventually turbulence generation and consequential turbulent mixing and plume dispersion and dilution. Therefore, dispersion of the dense gas plume is controlled by entertainment of ambient air through the leading edge and top surface of the plume.

Britter and McQuaid (1988) provide an empirical methodology to predict the transport of a dense gas and its subsequent dilution due to dispersion based upon dimensionless groups of variables and correlations obtained from experimental data (see Section 4). The goal of their analysis is to allow predictions of useful measures of dense gas dispersion to within a "factor of two." The primary dimensionless number relevant to the advection and dispersion of a dense gas such as CO_2 is the Richardson number, which is the ratio of buoyant forces stabilizing the flow to inertial forces that tend to disperse the flow. A convenient form of Ri for our purposes is

$$Ri = \frac{g' V_0^{1/3}}{u*^2} \qquad (5.4).$$

where V_0 is the volume of gas released. From the definition of g' (Eq. 4.2), the sign of Ri distinguishes stable and unstable density stratification. Specifically, for $Ri > 0$ the density contrast is stabilizing as occurs when CO_2 flows over the ground surface, while for $Ri < 0$ the density contrast is destabilizing as would occur when a light gas such as CH_4 flows over the ground surface. Puttock et al. (1982) found that for $Ri > 10$, density effects cannot be ignored and the dense gas dispersion is active as opposed to passive.

Britter and McQuaid (1988) also provide a brief review of the methods used in mathematical modeling of dense gas dispersion. They classify these models as "box", "intermediate (or slab)" and "three-dimensional (3D)". The basis for these categories is the manner by which the models represent the distribution of properties within the cloud. Box models assume that all properties are distributed uniformly over the volume of the cloud or a transverse slice of the plume. Three-dimensional models retain spatial discretization of properties in all three coordinate directions. Intermediate models apply some kind of spatial averaging in the vertical direction and thus fall between the other two types in their complexity.

Both the box and intermediate models make extensive use of correlations and dimensionless numbers identified in Britter and McQuaid (1988) to enable spatial averaging of properties within the plume volume. In fact, a large body of literature exists developed by the Petroleum Environmental Research Forum (PERF) based upon dense gas dispersion experiments conducted at the Fluid Modeling Facility (FMF) of the U.S. Environmental Protection Agency (EPA), the Chemical Hazards Research Center (CHRC) of the University of Arkansas, and the Environmental Flow Research Center (EnFlo) of the University of Surrey (Robins et al., 2001a; Robins et al., 2001b; Hanna and Chang, 2001; Hanna and Steinberg, 2001; Snyder, 2001; Briggs et al., 2001; Havens et al., 2001). These experiments are almost exclusively designed to substantiate correlations used in intermediate models such as HEGADAS (Witlox, 1994), DEGADIS (Spicer and Havens, 1989) and SLAB (Ermak, 1990). Ermak et al. (1982) describe the formulation and assumptions behind the Germeles-Drake (GD) modified Gaussian plume model (Germeles and Drake, 1975) which fits the box model category, and a modified version of Zeman's one-dimensional slab-averaged conservation model (Zerman, 1980) which constitutes the widely-used SLAB model and fits the intermediate model category. Both the GD and SLAB models were used to simulate the Burro series of experiments conducted at China Lake, CA (Ermak et al., 1982), including eight liquefied natural gas (LNG) tests with spill volumes of up to 40 m^3 and spill rates of up to 20 $m^3\ min^{-1}$ (0.33 $m^3\ s^{-1}$).

The 3D models represent a significant departure from the empirical methodology established by Britter and McQuaid (1988) in that they involve the rigorous solution of the three-dimensional Navier-Stokes with a generalized anelastic approximation. These include equations for the conservation of mass, momentum, energy and species. Ermak et al. (1982) present the FEM3 model which is based on this approach, and describe all equations and assumptions inherent in the formulation. Of particular note is their use of empirical correlations to enable closure of turbulence induced dispersion within the momentum, energy and species conservation equations. These dispersion terms were similar to those introduced in their SLAB model and were necessary

in order to model the high release rates of LNG emitted during the Burro series of experiments. A similar 3D model was developed by Macedonio and Costa (2002) in order to model advection and dispersion of CO_2 emitted from the ground surface in a situation typical of high CO_2 emission vents in Italy (Rogie et al., 2000). In this case, they employ the Smagorinski model for closure of turbulence-induced dispersion in the momentum equation. Their choice of turbulence closure model reflects the small-scale size of their model where a dense plume of CO_2 was transported a short distance of 20 m whereas Ermak et al. (1982) used FEM3 to model transport of LNG over distances of up to 400 m.

5.4 Modification of TOUGH2 for Modeling Atmospheric Dispersion

We present in this section a discussion of the potential use of the TOUGH2 framework (Pruess et al., 1999) to develop a coupled subsurface-surface layer simulation capability. The use of TOUGH2/EOS7CA to simulate atmospheric advection and dispersion of CO_2 begins by creating a logarithmic wind profile within the TOUGH2 framework. This step involves generating a grid in which both subsurface and surface layer regions conform to the topography of interest as shown on Figure 5.1. Sufficient layers are needed above the ground surface to discretize the wind profile to the desired accuracy. Next, a static gas phase pressure profile and constant pressure difference is applied between the upstream and downstream boundaries of the surface layer

$$\Delta P = P_2 - P_1, \quad P_1 > P_2 \tag{5.5}$$

where P_1 and P_2 are the upstream and downstream pressures, respectively. TOUGH2 computes the phase velocity using Darcy's equation

$$u = -\frac{k_D}{\phi \mu} \nabla \left(P - \rho g z \right) \tag{5.6}$$

where k_D is the intrinsic permeability, ϕ is the porosity, μ is the viscosity, ρ is the mass density of the gas phase, g is the gravitational acceleration and z is the elevation. Therefore, the velocity of the atmospheric air will be proportional to the permeability of the layer and pressure difference, ΔP. Given that ΔP is a constant for all layers, the individual permeability variations of the layers will combine to produce the logarithmic wind profile. This profile can be controlled by careful selection of layer permeability to create a logarithmic wind profile. Note that the thickness of each layer must be constant to ensure a constant air velocity within the layer across the length of the domain. Note further that the permeability is a pseudo-permeability with no physical significance; its purpose is to create the desired velocity profile.

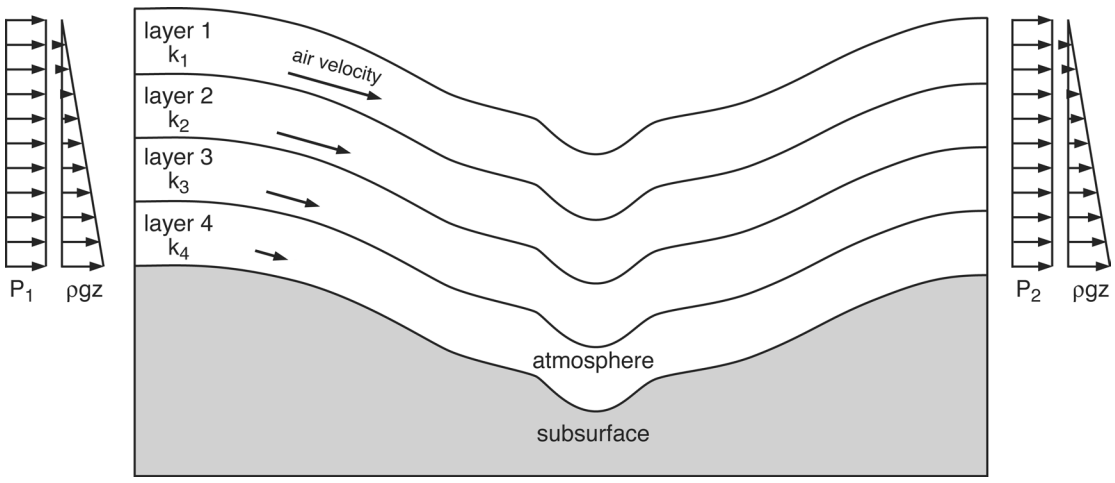

Figure 5.1. Conceptual method of discretizing the atmosphere into layers of varying permeability to enforce a logarithmic wind profile.

Transport of CO_2 can occur both as a dense or as a passive gas. Within the context of the TOUGH2 framework, transport of CO_2 as a passive gas will follow the linear advection-dispersion transport processes already used to calculate the transport of species within the gas phase. Ambient atmospheric dispersion of CO_2 using either P-G diffusion curves or the Smagorinski Model modified for the dispersion of a scalar can easily be implemented by spatially modifying molecular diffusion of CO_2 within the TOUGH2 surface layer grid. Specifically, the diagonal of the tensor representing Fickian diffusion of CO_2 would become the sum of molecular diffusion, as well as D_{xx} and D_{zz} from the P-G curves, as well as a contribution from the Smagorinski Model. This would enable TOUGH2/EOS7CA to estimate correctly the dispersion of the CO_2 plume due to both small- and large-scale eddies in the convective motion of the atmosphere.

Transport of CO_2 as a dense plume within the TOUGH2 framework is also relatively straight-forward. TOUGH2/EOS7CA solves a fully coupled set of equations representing the conservation of water, brine, CO_2, a gas tracer, air and energy, but does not solve a conservation of momentum equation. It does, however, implicitly describe the density-driven advection of a phase due to buoyant forces within Darcy's equation, which is used to compute the gas phase velocity. In this case, the gas phase mass density is a function of the mass fraction of components within the phase. Due to the use of Darcy's equation, advective–dispersive transport of the dense CO_2 plume will be proportional to the permeability of the layers used to enforce the ambient wind profile. Modeling conservation of momentum is needed to simulate spills of liquefied natural gas (LNG) at spill rates of up to 0.3 $m^3\ s^{-1}$ (20 $m^3\ min^{-1}$) for volumes of 40 m^3. Seepage of CO_2 from leaking geologic carbon sequestration sites to the surface layer would be at rates orders–of–magnitude less than that of LNG spills. Consequently, momentum-driven advection may not be important in the context of the seepage of CO_2 from leakage upward through lithologic layers overlying geologic carbon sequestration target formations.

Dispersive transport of a dense CO_2 plume can be modeled by the approach used in FEM3 (Ermak et al., 1982) or using the Smagorinski model as applied by Macedonio and Costa (2002). The latter is the simplest approach in that it requires no further modification to TOUGH2/EOS7CA beyond the work needed to implement dispersion of CO_2 as a passive gas. In fact, Macedonio and Costa (2002) show that for high seepage rates of CO_2 across small areas, the dense plume stays relatively close to the ground surface and is quickly diluted by small scale eddy diffusion as represented by the Smagorinski Model. As the surface area over which CO_2 seepage occurs becomes much larger, the resulting dense CO_2 plume may become influenced by larger scale eddy-diffusion mixing with the surrounding air, as well as entrainment of atmospheric air into the leading edge of the plume. These processes are implemented within FEM3 and can be incorporated into the TOUGH2 framework as a dispersion process using a diagonal dispersion tensor where:

$$D_{zz} = D_1(1 - X_g^{CO2}) + D_2 X_g^{CO2} \tag{5.7}$$

where X_g^{CO2} is the mass fraction of CO_2 in the gas phase, D_1 is dispersion due to eddy-diffusion mixing and D_2 is dispersion due to entrainment mixing. Dispersion due to eddy-diffusion mixing is given by Ermak et al. (1982) as:

$$D_1 = \frac{k\, u_* z}{\phi *} \tag{5.8}$$

where k is von Karman's constant (~0.4), $u*$ is the friction velocity, z is the elevation, and $\phi *$ is given by:

$$\phi^* = \begin{cases} (1 - 16Ri)^{-1/4}, & Ri \le 0 \\ 1 + 5Ri, & Ri > 0 \end{cases} \tag{5.9}$$

where Ri is the Richardson number. Entrainment mixing will occur with dispersion given by Ermak et al. (1982) as:

$$D_2 = \frac{1.25\rho(u_*)^3}{g(\rho - \rho_a)} \tag{5.10}$$

where ρ is the density of the plume, ρ_a is the ambient density of the air, and u_* is the friction

velocity. Finally,

$$D_{xx} = D_{yy} = 6.5 D_{zz} \tag{5.11}$$

which completes the discussion of advective and dispersive transport processes of a dense CO_2 plume within the TOUGH2 framework.

In summary, the design of the coupled subsurface-surface layer CO_2 flow and transport model involves the assumption of an average logarithmic wind velocity profile and the use of dispersion coefficients to model mixing due to small- and large-scale eddies. This is the standard approach used in atmospheric dispersion modeling. What is new in our approach is the explicit consideration of density effects and the coupling to the subsurface region. These latter features are required when modeling the fate and transport of a dense gas such as CO_2 seeping out from—but also possibly back into—the vadose zone. While our approach is standard for the case of passive mixing, considerable testing will be necessary to determine the range of applicability for cases of active dense gas mixing.

5.5 Test Problem

In this section, we present the most recent simulation test results for a problem of surface layer dispersion of CO_2 being emitted with non-zero velocity into a flow field with a logarithmic velocity profile. The verification problem is the CO_2 seepage case initially presented in Macedonio and Costa (2002) where dispersion of CO_2 is calculated using the Smagorinski Model. We compare our results with the Navier-Stokes solutions of Macedonio and Costa (2002), and with the results of VarDen, a variable density Navier-Stokes flow code (Almgren et al., 1998).

The Smagorinski Model from Macedonio and Costa (2002)

This test problem considers the subaerial transport of a cold CO_2 plume originating from a CO_2 vent at the ground surface. Macedonio and Costa (2002) originally solved this problem using the full Navier-Stokes equations with the Smagorinski Model for closure of turbulence-induced dispersion of momentum, heat, and CO_2. The problem schematic is sketched in Figure 5.2 and consists of a simple two-dimensional vertical cross-section 20 m long, 2 m high and of unit (1 m) width. Carbon dioxide is emitted along the bottom from a small area 2 m long, with a vertical velocity of 0.03 m s^{-1} and temperature of 13 °C. Thus the emission flow rate is 0.11 m^3 s^{-1}. The ambient temperature is 20 °C, hence the CO_2 plume is denser than the ambient air by virtue of both temperature and composition. The ambient wind in the system has a logarithmic velocity profile with wind speed of 3.25 m s^{-1} at the top of the domain and essentially zero at the ground surface. For the TOUGH2/EOS7CA simulation, we discretized the domain into 40 x 1 x 20 gridblocks of size 0.5 m x 1 m x 0.1 m, in the x-, y- and z-directions, respectively.

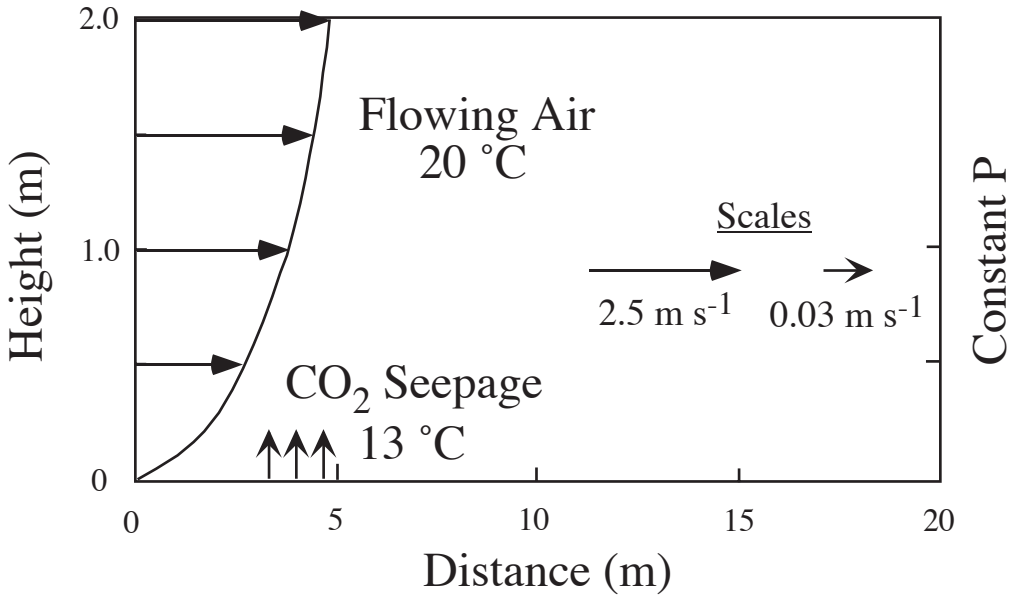

Figure 5.2. Schematic of Macedonio and Costa (2002) CO_2 dispersion problem.

A comparison of results at t = 40 s is presented in Figure 5.3. In Figure 5.3a, we have plotted shaded contours of normalized density, ρ^* ($\rho^* = (\rho-\rho_{air})/(\rho_{CO2}-\rho_{air})$) to compare with the VarDen results of Figure 5.3b, which shows shaded contours of the mass fraction of the advected scalar. Note that the VarDen solution is isothermal, with the advected scalar coded to produce the same density contrast as the combination of CO_2 and temperature in the original problem. Hence, the scalar in VarDen is representing the combination of thermal and compositional buoyancy effects, and is effectively the same as our normalized density (ρ^*). We present only contours of the mass fraction of CO_2 computed by Macedonia and Costa in Figure 5.3c as neither temperature, density, nor velocity data were presented in their paper (Macedonio and Costa, 2002). We set an artificially high thermal conductivity to make heat disperse through the system at approximately the same rate as CO_2. This was done to match the Macedonio and Costa (2002) approach, wherein they did not solve a thermal energy equation, but rather advected and dispersed heat in lockstep with CO_2.

Comparison of the three results shows broad similarities, but also distinct differences. In terms of similarity, the dense CO_2 gas tends to stay at the bottom of the system and is generally advected and dispersed downwind. However, the TOUGH2/EOS7CA result shows the density-driven flow to the left (upstream) occurs and leads to a recirculation and CO_2 in the lower left part of the domain. The VarDen results also show recirculation near the source, although to a lesser degree. The Maceodonio and Costa result shows no such recirculation. The VarDen result shows detailed flow structures not calculated by the other two models. Our preliminary assessment of this comparison is that inertial effects are important in the case where CO_2 emission occurs with finite velocity as in this problem, and the two Navier-Stokes simulations are capturing these effects, while the TOUGH2/EOS7CA result is not. We will continue to investigate the origins of the disparity in these results, and compare results for additional test problems.

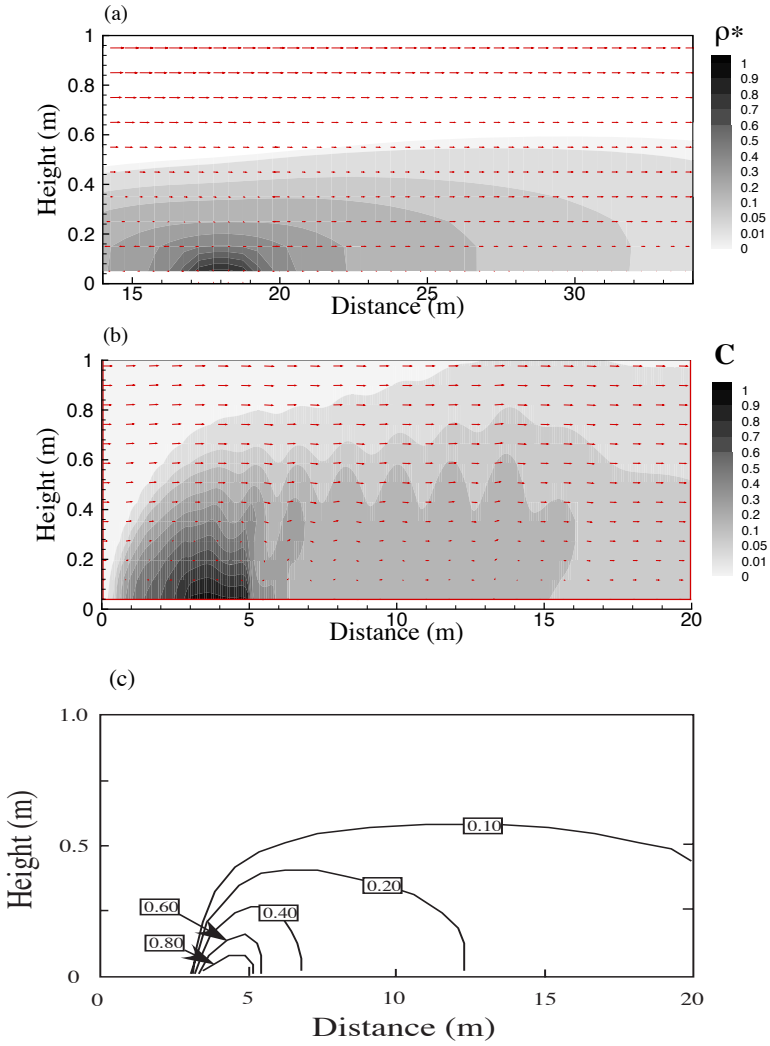

Figure 5.3. Comparison of results after 40 s for the CO_2 dispersion problem from (a) TOUGH2/EOS7CA; (b) VarDen; and (c) Macedonio and Costa (2002).

6. CONCLUSIONS

Atmospheric transport and dispersion of CO_2 in the surface layer and subaerial region is key to HSE risk assessment because these processes are capable of both bringing CO_2 to sensitive receptors, as well as diluting it to nonhazardous concentrations. As a denser and less viscous gas than ambient air, CO_2 can be expected to be mobile and ground-hugging. Such dense-gas flow behavior has been observed many times in nature as CO_2 has come out of the ground and travelled downslope often with disasterous consequences. HSE risk assessment for dense industrial gases has led to considerable work on dense gas dispersion that is directly applicable to CO_2 seepage from leaking carbon sequestration sites. In particular, the correlations derived from field and laboratory experiments can be applied to estimate flow characteristics of CO_2 seepage. Using these correlations, we have come up with the following results for CO_2 seepage with areal source length scale of 180 m over flat land with sparse vegetation and no buildings:

- CO_2 seepage at rates on the order of 1 m^3 s^{-1} will tend to spread nearly 1 km under calm conditions in a one-hour period. If there are winds present, entrainment of ambient air will lead to extensive dispersion and dilution of the plume after a few hundred meters of travel downwind. The plume is predicted to be approximately as wide at the downwind end as it is long for winds of 1–5 m s^{-1} measured at an elevation of 10 m.
- CO_2 seepage at rates on the order of 0.1 m^3 s^{-1}, as investigated in Task 1 of this project, is expected to spread several hundreds meters in an hour under calm conditions. With winds of 1–5 m s^{-1} at 10 m elevation, CO_2 concentrations would be orders of magnitude smaller than initial concentrations approximately 100 m downwind, and the plume at this location would be twice as wide as it is long.
- At the smaller seepage rates (e.g., ~0.01 m^3 s^{-1}) investigated in Task 1 of this project, nearly complete dilution occurs after tens of meters of travel downwind, making HSE risks small to receptors present above ground.

The above results suggest atmospheric dispersion is very effective, a result that needs to be rationalized in light of the numerous examples of lethal natural CO_2 emissions. Clearly, additional factors such as topography and calm conditions can inhibit dispersion and dilution. We will use a modeling approach that can consider density-driven flow, atmospheric dispersion and topographic effects. This approach will allow more defensible conclusions regarding HSE risk assessments to be made than is currently possible. Preliminary simulation results for CO_2 dispersion above ground show that more testing and development are needed.

ACKNOWLEDGMENTS

We thank Ann Almgren (LBNL) for carrying out VarDen simulations, and Marcelo Lippmann and Norm Miller (LBNL) for constructive comments and reviews of this report. This work was supported in part by a Cooperative Research and Development Agreement (CRADA) between BP Corporation North America, as part of the CO_2 Capture Project (CCP) of the Joint Industry Program (JIP), and the U.S. Department of Energy (DOE) through the National Energy Technologies Laboratory (NETL), and by the Ernest Orlando Lawrence Berkeley National Laboratory, managed for the U.S. Department of Energy under contract DE-AC03-76SF00098.

REFERENCES

Allard, P., Endogenous magma degassing and storage at Mount Etna, *Geophys. Res. Lett., 24(17),* 2219-2222, 1997.

Allard, P., D. Daljlevic, and C. Delarue, Origin of carbon dioxide emanation from the 1979 Dieng eruption, Indonesia: Implications for the origin of the 1986 Nyos catastrophe, in *The Lake Nyos event and natural CO_2 degassing, I,* edited by F. Le Guern and G.E. Sigvaldason, *Special Issue, J. Volcanol. Geotherm. Res., 39(2-3),* 195-206, 1989.

Allis R., T. Chidsey, W. Gwynn, C. Morgan, S. White, M. Adams, and J. Moore, Natural CO_2 reservoirs on the Colorado Plateau and Southern Rocky Mountains: Candidates for CO_2 Sequestration, in *Proceedings of the First National Conference on Carbon Sequestration*, National Energy Technology Laboratory, US Department of Energy, Washington, D.C., May 14-17, 2001.

Allison, M. L., 2001, Hutchinson, Kansas: a geologic detective story; *Geotimes*,*46*(10), 14-20, October, 2001

Almgren, A.S., J.B. Bell, P. Colella, L.H. Howell, and M.L. Welcome, A conservative adaptive projection method for the variable density incompressible Navier-Stokes equations, *J. Comput. Phys.*, *142*, 1–46, 1998.

Arya, S.P., *Air Pollution Meteorology and Dispersion*, Oxford University Press, 1999.

Baldocchi, D.D. and K.B. Wilson, Modeling CO2 and water vapor exchange of a temperate broadleaved forest across hourly to decadal time scales, *Ecological Modelling*, *142*, 155-184, 2001.

Barberi, F., W. Chelini, G. Marinelli, and M. Martini, The gas cloud of Lake Nyos (Cameroon, 1986): Results of the Italian technical mission, in *The Lake Nyos event and natural CO_2 degassing, I,* edited by F. Le Guern and G.E. Sigvaldason, *Special Issue, J. Volcanol. Geotherm. Res., 39(2-3),* 125-134, 1989.

Barbier, E., Nature and technology of geothermal energy: A review, *Renewable and Sustainable*

Energy Reviews, 1(1-2), 1-69, 1997.

Baubron, J.C., P. Allard, and J.P. Toutain, Diffuse volcanic emissions of carbon dioxide from Vulcano Island, Italy, *Nature, 344*, 51-53, 1990.

Baxter, P.J. and M. Kapila, Acute health impact of the gas release at Lake Nyos, Cameroon, 1986, in *The Lake Nyos event and natural CO_2 degassing, I,* edited by F. Le Guern and G.E. Sigvaldason, *Special Issue, J. Volcanol. Geotherm. Res., 39(2-3),* 265-275, 1989.

Briggs, G.A., R.E. Britter, S.R. Hanna, J.A. Havens, A.G. Robins and W.H. Snyder, Dense gas vertical diffusion over rough surfaces: Results of wind-tunnel studies., *Atmospheric Environment*, *35*, 2265-2284, 2001.

Britter, R.E., Atmospheric dispersion of dense gases, *Ann. Rev. Fluid Mech.*, *21*, 317–344, 1989.

Britter R.E., and R.F. Griffiths, editors, *Dense Gas Dispersion*, Chemical Engineering Monographs 16, Elsevier, New York, 1982.

Britter, R.E and J. McQuaid. *Workbook on the Dispersion of Dense Gases*. Health Saf. Exec. Rep., Sheffield, UK, HSE Contract Research Report No. 17/1988, 1988.

Brown, K.L., Occupational safety and health, in *Environmental Aspects of Geothermal Development*, convened by K.L. Brown, International Geothermal Association, Inc., Auckland, NZ, 119-130, 1995.

Chafetz, H.S., P.F. Rush, and N.M. Utech, Microenvironmental controls on meneralogy and habit of $CaCO_3$ precipitates: An example from an active travertine system, *Sedimentology, 38*, 107-126, 1991.

Cramer, S.D., The solubility of methane, carbon dioxide, and oxygen in brines from 0 ˚ to 300 ˚C, *U.S. Bureau of Mines: Report No. 8706*, 16 pp., 1982.

D'Allessandro, W., S. Giammanco, F. Parello, and M. Valenza, CO_2 output and $\delta^{13}C(CO_2)$ from Mount Etna as indicators of degassing of shallow asthenosphere, *Bull. Volcanol., 58*, 455-458, 1997.

Duchi, V., A.A. Minissale, and F. Pratt, Chemical composition of thermal springs, cold springs, streams, and gas vents in the Mt. Amiata geothermal region (Tuscany, Italy), *J. Volcanol. Geotherm. Res., 31*, 321-332, 1987.

Ellis, A.J. and W.A.J. Mahon, *Chemistry and Geothermal Systems*, Academic Press, New York, NY, 392 pp., 1977.

Ermak, D.L., User's manual for SLAB: An atmospheric dispersion model for denser-than-air releases, Lawrence Livermore National Laboratory, Livermore, CA, *Report UCRL-MA-105607*, , 1990.

Ermak, D.L., S.T. Chan, D.L. Morgan and L.K. Morris, A comparison of dense gas dispersion model simulations with Burro Series LNG Test results, *Journal of Hazardous Materials*, *6*, 129-160, 1982.

Evans, W.C., L.D. White, M.L.Tuttle, G.W. Kling, G. Tanyileke, and R.L. Michel, Six years of change at Lake Nyos, Cameroon, yield clues to the past and cautions for the future, in

Geochemistry of Crater Lakes, edited by M. Kusakabe, *Special Issue, Geochemical J., 28*, 139-162, 1994.

Farrar, C.D., J.M. Neil and J.F. Howle., Magmatic carbon dioxide emissions at Mammoth Mountain, California, *U.S. Geological Survey Open-File Report* 98-4217, 34 pp. and 1 plate, 1999.

Farrar, C.D., M.L. Sorey, W.C. Evans, J.F. Howle, B.D. Kerr, B.M. Kennedy, C.-Y. King and J.R. Southon., Forest-killing diffuse C)2 emissions at Mammoth Mountain as a sign of magmatic unrest, *Nature*, *376* (6542), p. 675-678, 1995.

Faivre-Pierret, R.X., P. Berne, C. Roussel, and F. Le Guern, The Lake Nyos disaster: Model calculations for the flow of carbon dioxide, *J. Volcanol. Geotherm. Res., 51*, 161-170, 1992.

Gerlach, T.M., Etna's greenhouse pump, *Nature, 351*, 352-353, 1991.

Germeles, A.M. and E.M. Drake, Gravity spreading and atmospheric dispersion of LNG vapor clouds, 4th International Symp. On Transport of Hazardous Cargoes by Sea and Inland Waterways, Jacksonville, FL, Oct. 1975.

Gifford, F.A. Jr., Use of routine meterological observations for estimating atmospheric dispersions, *Nuclear Safety*, *2*, 47– , 1961.

Graziani, G., A. Martilli, M.T. Pareschi, and M. Valenza, Atmospheric dispersion of natural gases at Vulcano Island, *J. Volcanol. Geotherm. Res., 75*, 283-308, 1997.

Hanna, S.R. and K.W. Steinberg, Overview of Petroleum Environmnetal Research Forum (PERF) dense gas dispersion modeling project., *Atmospheric Environment*, *35*, 2223-2229, 2001.

Hanna, S.R. and J.C. Chang, Use of the Kit Fox field data to analyze dense gas dispersion modeling issues., *Atmospheric Environment*, *35*, 2231-2242, 2001.

Havens, J. H. Walker and T.O. Spicer, Wind tunnel study of air entrapment into two-dimensional dense gas plumes at the Chemical Hazards Research Center, *Atmospheric Environment*, *35*, 2305-2317, 2001.

Hill, P.M., Possible asphyxiation from carbon dioxide of a cross-country skier in eastern California: A deadly volcanic hazard, *Wilderness and Environmental Medicine, 11(3),* 192-195, 2000.

Holloway, M., The killing lakes, *Scientific American, 283(1),* 92-99, 2000.

Le Guern, F., E. Shanklin, and S. Tebor, Witness accounts of the catastrophic even of August 1986 at Lake Nyos (Cameroon), *J. Volcanol. Geotherm. Res., 51*, 171-184, 1992.

Le Guern, F., H. Tazieff, and R. Faivre Pierret, An example of health hazard: People killed by gas during a phreatic eruption: Dieng Plateau (Java, Indonesia), February 20th, 1979, *Bull. Volcanol., 45(3),*153-156, 1982.

Macedonio, G. and A. Costa, Finite element modeling of gas dispersion in the atmosphere., in Proc. Arezzo Seminar in Fluids Geochemistry. Buccianti A., Marini L., Ottonello G. and Vaselli O. Eds Pacini Editore, Ospedaletto (PISA) p. 147-159, 2002.

Magee, J.W., J.A. Howley, and J.F. Ely, "A predictive model for the thermophysical properties of carbon dioxide rich mixtures," *Research Report RR-136*, Gas Processors Assoc., Tulsa OK, 35 pp., 1994.

NIST (National Institute of Science and Technology), *NIST Database 14 Mixture Property Database, version 9.08*, U.S. Department of Commerce (Oct. 1992).

Oldenburg, C.M., A.J.A. Unger, R.P. Hepple, and P.D. Jordan, On Leakage and Seepage from Geologic Carbon Sequestration Sites, Lawrence Berkeley National Laboratory Report *LBNL-51130*, July 2002a.

Oldenburg, C.M., T.E. McKone, R.P. Hepple, and A.J.A. Unger, Health Risks from Leakage and Seepage of CO_2 Sequestered in the Subsurface: Requirements and Design of a Coupled Model for Risk Assessment, Lawrence Berkeley National Laboratory Report *LBNL-51131*, July 2002b.

Pasquier-Cardin, A., P. Allard, T. Ferreira, C. Hatte, R. Coutinho, M. Fontugne, and M. Jaudon, Magma-derived CO_2 emissions recorded in ^{14}C and ^{13}C content of plants growing in Furnas caldera, Azores, *J. Volcanol. Geotherm. Res., 92*, 195-207, 1999.

Pasquill, F., The estimation of the dispersion of windborne material, *Meterological Magazine*, *90*, 33–49, 1961.

Pasquill, F., *Atmospheric Diffusion*, John Wiley and Sons, Chichester, England, 2nd edition, 1974.

Pentecost, A., The formation of travertine shrubs: Mammoth Hot Springs, Wyoming, *Geol. Mag., 127(2),* 159-168, 1990.

Pentecost, A., The Quaternary travertine deposits of Europe and Asia Minor, *Quaternary Sci. Rev., 14*, 1005-1028, 1995.

Pruess, K., C. Oldenburg, and G. Moridis, TOUGH2 User's Guide Version 2.0, Lawrence Berkeley National Laboratory Report *LBNL-43134*, 197 pp., November 1999.

Reid, Jr., J.B., J.L Reynolds, N.T. Connolly, S.L. Getz, P.J. Polissar, L.J. Winship, and L.J. Hainsworth, Carbon isotopes in aquatic plants, Long Valley caldera, California as reconds of past hydrothermal and magmatic activity, *Geophys. Res. Lett., 25(15),* 2853-2856, 1998.

Robins, A., I. Castro., P. Hayden, N. Steggel, D. Contini and D. Heist, A wind tunnel study of dense gas dispersion in a neutral boundary layer over a rough surface., *Atmospheric Environment*, *35*, pp 2243-2252, 2001a.

Robins, A., I. Castro., P. Hayden, N. Steggel, D. Contini, D. Heist, and T.J. Taylor, A wind tunnel study of dense gas dispersion in a stable boundary layer over a rough surface., *Atmospheric Environment*, *35*, pp 2253-2263, 2001b.

Rogie, J.D., D.M. Kerrick, M.L. Sorey, G. Chiodini, and D.L. Galloway, Dynamics of carbon dioxide emission at Mammoth Mountain, California, *Earth and Planetary Sci. Letters*, *188*, 535–541, 2001.

Rogie, J.D., D.M. Kerrick, G. Chiodini, and F. Frondini, Flux measurements of nonvolcanic CO_2 emission from some vents in central Italy, *J. Geophys. Res.*, *105*(B4), 8435–8445, 2000.

Simkin, T., and L. Siebert, *Volcanoes of the World*, Smithsonian Institution and Geoscience Press, Inc., Tucson, Arizona, 349p., 1994.

Slade, D.H., (editor), *Meteorology and Atomic Energy 1968*, Chapter 2, U.S. Atomic Energy Commission, 1968.

Smithsonian Institute (SI), Global Volcanism Program, 2001. http://www.volcano.si.edu/gvp/index.htm

Snyder, W.H., Wind-tunnel study of entrainment in two-dimensional dense-gas plumes at the EPA's fluid modeling facility, *Atmospheric Environment*, *35*, 2285-2304, 2001.

Sorey, M., B. Evans, M. Kennedy, J. Rogie and A. Cook, Magmatic gas emissions from Mammoth Mountain, *California Geology*, *52*(5), 4–16, 1999.

Spicer, T.O. and J.A. Havens, User's guide for the DEGADIS 2.1 dense gas dispersion model. *EPA-450/4-89-019*, USEPA, Research Triangle Park, NC, 27711 USA, 1989.

Stull, R.B., *An Introduction to Boundary Layer Meteorology*, Kluwer Academic Publishers, Dordrecht, The Netherlands, 666 pp., 1988.

Stupfel, M. and F. Le Guern, Are there biomedical criteria to assess an acute carbon dioxide intoxication by a volcanic emission?, in *The Lake Nyos event and natural CO_2 degassing, I,* edited by F. Le Guern and G.E. Sigvaldason, *Special Issue, J. Volcanol. Geotherm. Res., 39(2-3),* 247-264, 1989.

USGS, Carbon dioxide and helium discharge from Mammoth Mountain, *U.S. Geological Survey Volcano Hazards Program, Long Valley Observatory, on-line fact sheet*, 1999. http://lvo.wr.usgs.gov/CO2.html,http://quake.wr.usgs.gov/VOLCANOES/LongValley/CO2.html

Vargaftik, N.B., Y.K. Vinogradov, and V.S. Yargin, *Handbook of Physical Properties of Liquids and Gases, Third Edition*, Begell House, New York, 1359 pp., 1996.

Webster, J.G., Chemical impacts of geothermal development, in *Environmental Aspects of Geothermal Development*, convened by K.L. Brown, International Geothermal Association, Inc., Auckland, NZ, 79-95, 1995.

Witlox, H.W.M., The HEGADIS model for ground-level heavy-gas dispersion – I. Steady-state model., *Atmospheric Environment*, *28*, 2917-2932, 1994.

Zerman, O., The dynamics and modeling of heavier-than-air cold gas releases, Lawrence Livermore National Laboratory, Livermore, CA, *Report UCRL-15224*, April 1980.